ARL-TR-8934 • Apr 2020

DEVCOM ARMY RESEARCH LABORATORY

Optimizing the Performance of Aluminized Explosives: Laser-Based Measurements of Energy Release and Spectroscopic Diagnostics

by Jennifer L Gottfried, Steven W Dean, Chi-Chin Wu, and Frank C De Lucia, Jr

NOTICES

Disclaimers

The findings in this report are not to be construed as an official Department of the Army position unless so designated by other authorized documents.

Citation of manufacturer's or trade names does not constitute an official endorsement or approval of the use thereof.

Destroy this report when it is no longer needed. Do not return it to the originator.

ARL-TR-8934 ● APR 2020

Optimizing the Performance of Aluminized Explosives: Laser-Based Measurements of Energy Release and Spectroscopic Diagnostics

Jennifer L Gottfried, Steven W Dean, Chi-Chin Wu, and Frank C De Lucia, Jr
Weapons and Materials Research Directorate, CCDC Army Research Laboratory

REPORT DOCUMENTATION PAGE

Form Approved
OMB No. 0704-0188

1. REPORT DATE *(DD-MM-YYYY)*	2. REPORT TYPE	3. DATES COVERED (From - To)
April 2020	Technical Report	1 December 2018–31 July 2019

4. TITLE AND SUBTITLE
Optimizing the Performance of Aluminized Explosives: Laser-Based Measurements of Energy Release and Spectroscopic Diagnostics

5a. CONTRACT NUMBER

5b. GRANT NUMBER

5c. PROGRAM ELEMENT NUMBER

6. AUTHOR(S)
Jennifer L Gottfried, Steven W Dean, Chi-Chin Wu, and Frank C De Lucia, Jr

5d. PROJECT NUMBER

5e. TASK NUMBER

5f. WORK UNIT NUMBER

7. PERFORMING ORGANIZATION NAME(S) AND ADDRESS(ES)
CCDC Army Research Laboratory
ATTN: FCDD-RLW-LB
Aberdeen Proving Ground, MD 21005-5069

8. PERFORMING ORGANIZATION REPORT NUMBER
ARL-TR-8934

9. SPONSORING/MONITORING AGENCY NAME(S) AND ADDRESS(ES)

10. SPONSOR/MONITOR'S ACRONYM(S)

11. SPONSOR/MONITOR'S REPORT NUMBER(S)

12. DISTRIBUTION/AVAILABILITY STATEMENT
Approved for public release; distribution is unlimited.

13. SUPPLEMENTARY NOTES
ORCID ID(s): Jennifer Gottfried, 0000-0002-1282-1928

14. ABSTRACT
Commercial aluminum powders (nanometer- and micrometer-sized) have been thoroughly characterized by conventional analytical techniques to compare source and lot-to-lot variations in the material properties. The energy release rates of milligram-quantity samples ignited with a nanosecond-pulsed laser at heating rates on the order of 10^{13} K/s have been investigated by measuring the laser-induced shock wave velocities and tracking the formation of aluminum monoxide on both the microsecond and millisecond timescales. By comparing the material properties and resultant energetic behavior, new insights into the optimal properties have been achieved. Preliminary results from methods we are investigating to accelerate the oxidation of aluminum in explosive formulations for enhanced detonation performance are also discussed.

15. SUBJECT TERMS
laser ablation, aluminum, detonation performance, emission spectroscopy, explosives

16. SECURITY CLASSIFICATION OF:			17. LIMITATION OF ABSTRACT	18. NUMBER OF PAGES	19a. NAME OF RESPONSIBLE PERSON
a. REPORT	b. ABSTRACT	c. THIS PAGE			Jennifer L Gottfried
Unclassified	Unclassified	Unclassified	UU	22	19b. TELEPHONE NUMBER (Include area code) (410) 278-7573

Contents

List of Figures iv

Acknowledgments v

1. Introduction 1

2. Experimental 2

2.1 Samples 2

2.2 Analytical Characterization of Samples 2

2.3 LIBI Setup and Diagnostics 2

3. Influence of Aluminum Particle Properties on Oxidation Rates 4

3.1 Early-Time Energy Release 4

3.2 Middle-Time Energy Release 7

3.3 Late-Time Energy Release 8

4. Methods for Catalyzing Aluminum Oxidation 8

4.1 Metal Alloys 9

4.2 Passivating with Carbon 9

4.3 Coating with Oxygen-Containing Species 9

5. Conclusions 10

6. References 11

List of Symbols, Abbreviations, and Acronyms 14

Distribution List 15

List of Figures

Fig. 1 Experimental schematic of the LIBI setup for analyzing the microsecond- and millisecond-timescale energy release from laser-excited (~10^{13} K/s) Al powders 3

Fig. 2 Laser-induced shock velocities (normalized to the blank tape substrate) for nine commercial Al powders vs. the average measured particle size (via DLS or 2-laser diffraction). The percentages refer to the active Al content measured via TGA. 5

Fig. 3 TEM images of a) the best-performing nanopowder Al with the highest active Al content, b) the 91-nm Al with nanoflakes, and c) the 18-nm Al with nanorods 6

Fig. 4 Time-resolved AlO emission intensities for the nanopowder Al and <75 μm Al samples acquired with the ICCD spectrometer set to a 1-μs gate width and varying delay times (averaged over 20 laser shots at each delay time) 7

Fig. 5 Time to peak AlO emission intensities in the middle-energy release time regime as a function of specific surface area 8

Acknowledgments

The authors thank Trevor Tovar for performing the Brunauer–Emmett–Teller analysis, Lily Giri for obtaining scanning electron micros images, Elliot Wainwright for obtaining 2-laser diffraction measurements of the micrometer-sized aluminum samples, Frank Kellogg for the differential scanning calorimetry and thermogravimetric analysis (TGA) measurements, Alice Savage for her assistance with dynamic light scattering measurements, and Rose Pesce-Rodriguez for Fourier transform infrared and TGA analyses. This report is an extended version of a proceedings paper for an invited talk presented by Jennifer Gottfried at the 2019 IEEE RAPID conference in Miramar Beach, Florida, August 19–21, 2019.

1. Introduction

To improve the lethality of current military explosive formulations, novel metal additives for enhanced energy release are being investigated. Because of its high theoretical energy content when fully oxidized (up to 31 kJ/g compared to 14.5 kJ/g for trinitrotoluene [TNT]), aluminum (Al) is of significant interest for this application. Micrometer-sized Al (micron-Al) powder is currently used in military formulations such as tritonal (80% TNT + 20% Al) to enhance the total heat output, resulting in enhanced blast effects or increased bubble energy in underwater explosions. Since most of the Al reacts after the passage of the detonation wave, however, the detonation velocity of the explosive is decreased by the presence of the inert mass from the unreacted Al.[1] In addition, incomplete combustion of the Al due to agglomeration or sintering of the particles during heating results in significantly less energy output than the theoretical maximum.

Aluminum nanoparticles (nano-Al) react significantly faster than micron-Al since they have a much larger surface-to-volume ratio, but the presence of the native oxide layer (alumina, Al_2O_3) that forms spontaneously in air on unpassivated Al not only converts a substantial fraction of the nano-Al to parasitic mass, it delays the energy release by acting as a barrier to oxidation of the Al core. Severe particle aggregation in some nano-Al particles also reduces the available contact surfaces. Many potential solutions to these problems have been explored by various groups, but the complexity of scaling up to larger quantities of material and the expense of detonation testing have inhibited the development of aluminized explosives with improved performance. While nano-Al has been used to enhance burn rates in propellants,[2] the limited number of published reports of large-scale detonation testing of formulations containing nano-Al have produced conflicting results. Some researchers reported increases in detonation performance (i.e., detonation velocity or Gurney energy) with the use of nano-Al,[3,4] while many others reported no enhancement compared to micron-Al.[2,5,6]

To understand the influence of particle size and other properties on the fast (microsecond-timescale) and slow (millisecond-timescale) energy release from Al at the heating rates relevant to detonation events (~10^{13} K/s), commercial Al powders varying in size from a nominal 18 nm to less than 75 μm were excited with a nanosecond-pulsed laser. A modified experimental setup based on the laser-induced air shock from energetic materials (LASEM) technique[7,8] was used to characterize the energy release behavior of the Al particles. The laser-induced breakdown ignition (LIBI) experimental setup uses high-time-resolution LASEM to evaluate the microsecond-timescale energy release and numerous diagnostics to investigate the reactions of metal powders excited at high heating rates. Several

examples of methods for accelerating the microsecond-timescale energy release of Al particles are also discussed.

2. Experimental

2.1 Samples

Nine commercial Al powders were obtained from various vendors and colleagues at the US Army Combat Capabilities Development Command Army Research Laboratory (ARL). The different samples were in both unopened and opened containers and were either recently purchased or purchased many years ago. The synthesis and treatment methods, while not specified by the manufacturer, were also expected to vary significantly among the samples. Manufacturer-specified particle sizes on the sample labels were listed as 18 nm, 44 nm, 80 nm, 91 nm, "nanopowder", 1–2 μm, 3–4.5 μm, –325 mesh, and <75 μm. Samples for LIBI analysis were prepared by firmly pressing the Al powder into double-sided tape on a glass microscope slide to achieve residue thicknesses of approximately 1.3 mg/cm^2.

2.2 Analytical Characterization of Samples

To understand the differences in the properties of the Al powders, extensive analytical characterization of the samples was performed. For determination of particle sizes, dynamic light scattering (DLS), 2-laser diffraction, Brunauer–Emmett–Teller (BET) analysis, scanning electron microscopy (SEM), and transmission electron microscopy (TEM) were performed. BET was used to directly measure the specific surface area, and zeta-potentials were measured for several of the nano-Al samples. Fourier transform infrared (FTIR) spectroscopy was used to investigate the surface functional groups, and laser-induced breakdown spectroscopy (LIBS) provided information about the elemental composition of the samples (including metal and organic impurities). Active Al content was measured using differential scanning calorimetry and thermogravimetric analysis (DSC-TGA).

2.3 LIBI Setup and Diagnostics

The LIBI setup is based on the excitation of a thin layer of Al powder by a Nd:YAG laser pulse (850 mJ, 6 ns, 1064 nm) focused with a 10-cm lens to a point just below the sample surface (Fig. 1). Unlike the original LASEM setup, the LIBI setup uses a spoiled coherence laser (SILUX 640) as the illumination source for schlieren imaging the laser-induced shock wave as it expands into the air above the sample.

A bandpass filter at the illumination laser wavelength was placed in front of the high-speed monochrome camera (Photron SAZ) to reduce interference from the laser-induced plasma emission at early times. The imaging laser is capable of producing pulses of light as short as 10 ns, enabling shorter exposure times than can be obtained with the camera shutter (159 ns). The frame rate of the camera was set to 800,000 frames per second, increasing the time resolution of the original LASEM setup by nearly an order of magnitude. Although the LIBI setup has not been calibrated to estimate detonation velocities of explosives,[8] the measured laser-induced shock wave velocities still provide a qualitative comparison of the microsecond-timescale energy release of the ablated samples.

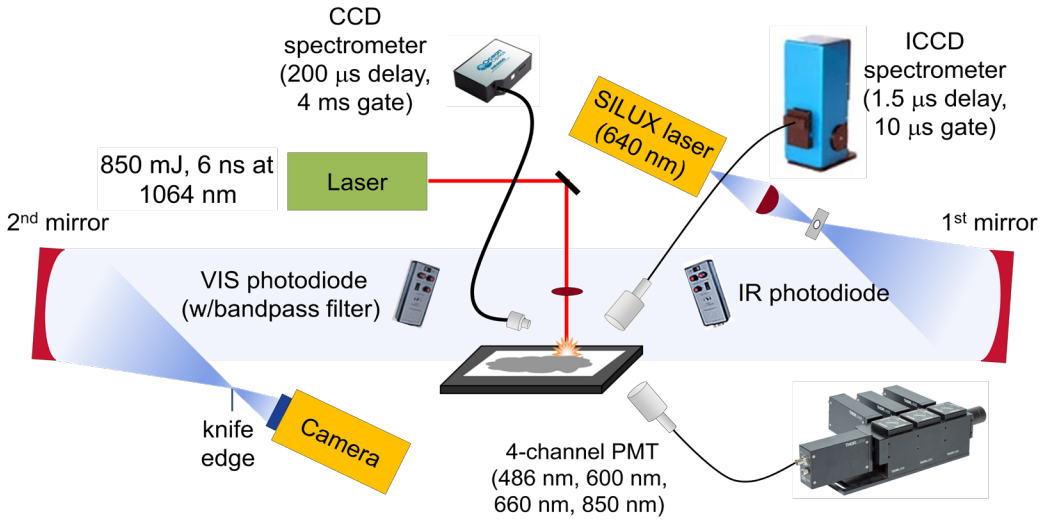

Fig. 1 Experimental schematic of the LIBI setup for analyzing the microsecond- and millisecond-timescale energy release from laser-excited (~10^{13} K/s) Al powders

In addition to measuring the laser-induced shock wave velocities, an echelle spectrograph with an intensified charge-coupled device (ICCD) detector was used to record the time-resolved emission from the reacting species in the laser-induced plasma (Catalina Scientific SE200, 200–1000 nm, 0.02-nm resolution). A 2-channel detector consisting of photomultiplier tubes (PMTs) with bandpass filters was used to record the emission from aluminum monoxide (AlO) (480 nm) and the blackbody emission (560 nm); the blackbody emission was subtracted from the AlO emission for background correction. Millisecond-timescale combustion emission was monitored with a gated CCD spectrometer (Ocean Optics HR4000, 230–900 nm, 0.25 nm), an infrared-sensitive photodiode (New Focus Model 2053, 900–1700 nm), and a visible-sensitive photodiode (New Focus Model 2051, 300–1050 nm). Two high-speed cameras (Phantom v7.3) provided the capability for either 2-color spatially resolved pyrometry (at 700 and 900 nm)[9] or high dynamic range imaging[10] of the laser excitation event.

While the amount of material contributing to the high-temperature plasma reactions on the microsecond-timescale is independent of the sample thickness,[11] the combustion emission strongly depends on the amount of material ejected from the sample surface. Therefore, the mass of the sample slide was measured before and after each laser shot to estimate the amount of reacted material. Mass loss after each laser shot reflects the combination of the ablated material that reacts in the laser-induced plasma, the material ejected off the sample slide that combusts in the air above the sample, and unreacted material ejected from the sample slide.

3. Influence of Aluminum Particle Properties on Oxidation Rates

Three distinct time regimes for Al oxidation and energy release have been observed with the LIBI experiment. At early times (0–10 μs), excited species reacting in the laser-induced plasma such as Al can produce exothermic reactions that increase the measured laser-induced shock velocity compared to that observed from inert materials at the same laser pulse energy. Since the laser-induced shock velocities measured from energetic materials have been shown to correlate to detonation velocities obtained from large-scale detonation testing,[8] materials that release more energy following laser excitation in this early-time regime are expected to react in the chemical reaction zone behind the detonation front. After 10 μs, the laser-induced shock wave has expanded into the air above the laser-induced plasma and quickly reaches the speed of sound in air. In this middle-time regime (10–500 μs), combustion of plasma-ignited particles can be observed with the PMTs. We speculate that the presence of AlO emission in this regime could be used to indicate the extent of exothermic reactions contributing to the Gurney velocity (i.e., metal acceleration) of a detonating explosive—although investigation of the reactions in this time regime is ongoing. Finally, at late times (1–200 ms) laser-induced deflagration reactions from the fast, self-sustained combustion of particles ejected from the sample slide into the air heated by the plasma and passage of the shock wave are observed.[12]

3.1 Early-Time Energy Release

The characteristic laser-induced shock velocities for the Al samples (Fig. 2) show that the four micron-Al powders (orange) have statistically identical microsecond-timescale energy release following laser excitation at high heating rates. While they are slightly exothermic compared to the blank tape substrate (y-axis value of 1), only a small fraction of the micron-Al reacts at this timescale—as shown from previous LASEM results[1] and confirmed with large-scale detonation tests. The

nano-Al samples (blue) have significantly more microsecond-timescale energy release. The average particle size of the nominally 80-nm sample measured with DLS was 845 nm (orange circle with blue outline). While the TEM images confirm the primary particle size of this sample was 60–100 nm, strong agglomeration of this sample resulted in the higher effective particle sizes from DLS. Sonication was sufficient to break up the agglomeration of the other nano-Al samples. Zeta-potential measurements confirmed that 80-nm sample has a much higher magnitude surface charge than the other nano-Al samples.

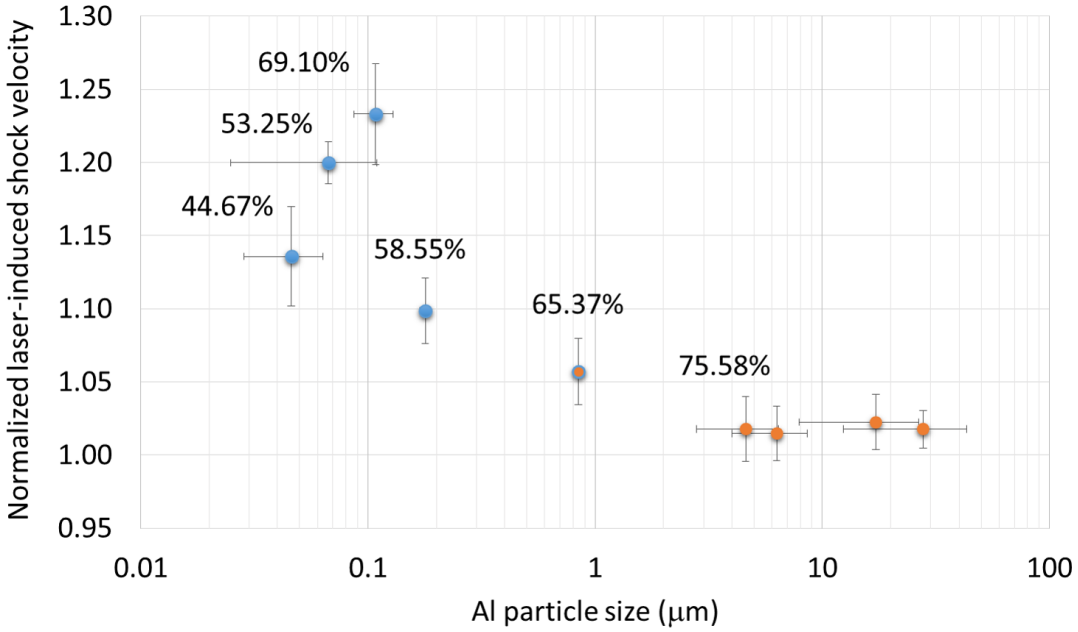

Fig. 2 Laser-induced shock velocities (normalized to the blank tape substrate) for nine commercial Al powders vs. the average measured particle size (via DLS or 2-laser diffraction). The percentages refer to the active Al content measured via TGA.

The microsecond-timescale energy release of the nano-Al samples depends not just on the particle size (or specific surface area), but also on the active Al content. The nanopowder Al sample had a measured average particle size of 108 nm (Fig. 3a) and the most significant microsecond-timescale energy release (Fig. 2), while the nominally 91-nm Al sample had an average particle size of 179 nm and a comparatively low microsecond-timescale energy release. The active Al content for the two samples was 69.10% and 58.55%, respectively. TEM images show that the 91-nm Al had spherical particles interspersed with small nanoflakes (Fig. 3b). The 18-nm Al, which had the lowest active Al content, contained numerous silicon-containing nanorods (Fig. 3c). These results demonstrate that particle size alone is not sufficient to predict microsecond-timescale energy release. Since the properties of nanoparticles are well-known to vary significantly from lot to lot, it is essential

to thoroughly characterize the particle morphology, impurities, and active Al content prior to testing as an energetic material additive.

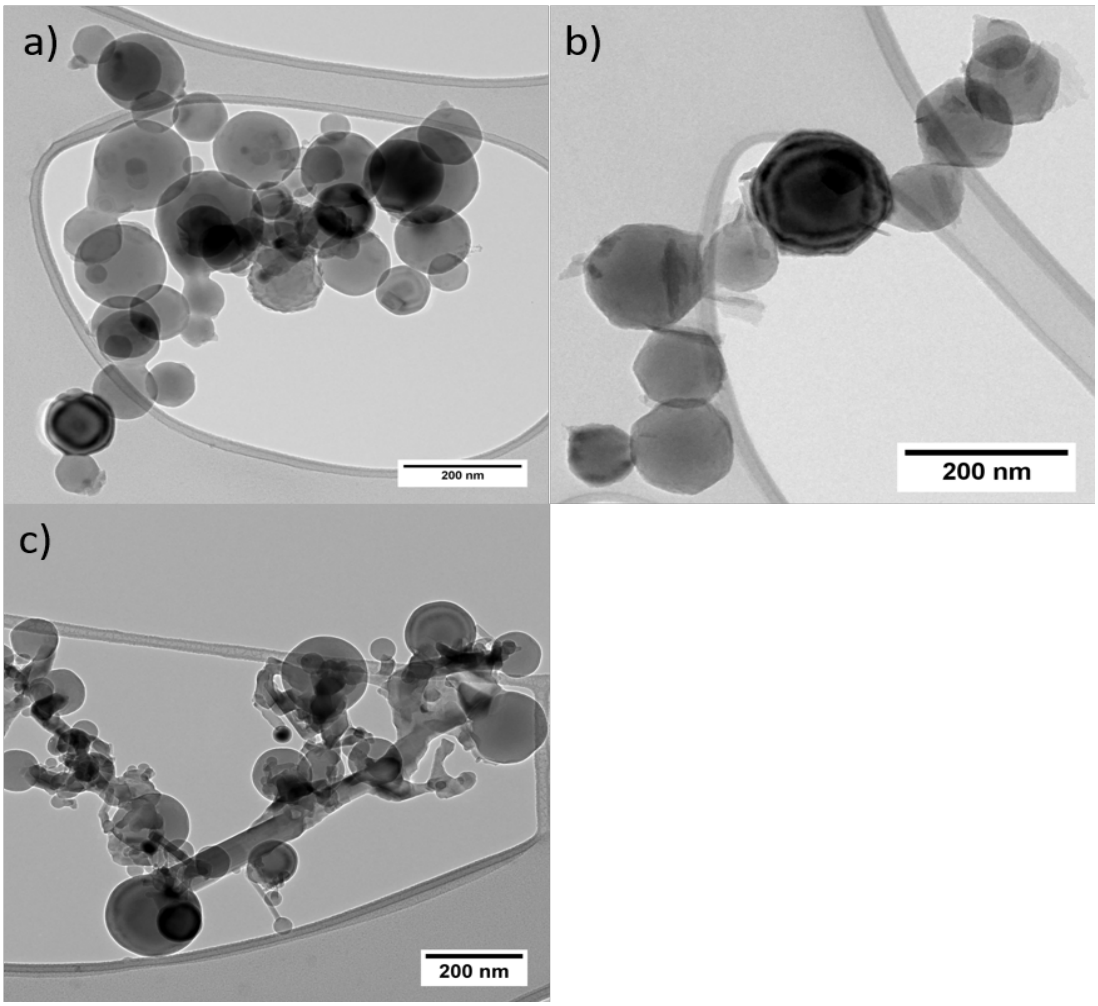

Fig. 3 TEM images of a) the best-performing nanopowder Al with the highest active Al content, b) the 91-nm Al with nanoflakes, and c) the 18-nm Al with nanorods

Time-resolved measurements of the AlO emission intensities during the first 10 μs confirm that the nano-Al samples undergo more significant oxidation on the microsecond-timescale than the micron-Al (Fig. 4). Peak AlO emission from the micron-Al does not occur until approximately 120 μs after laser excitation.

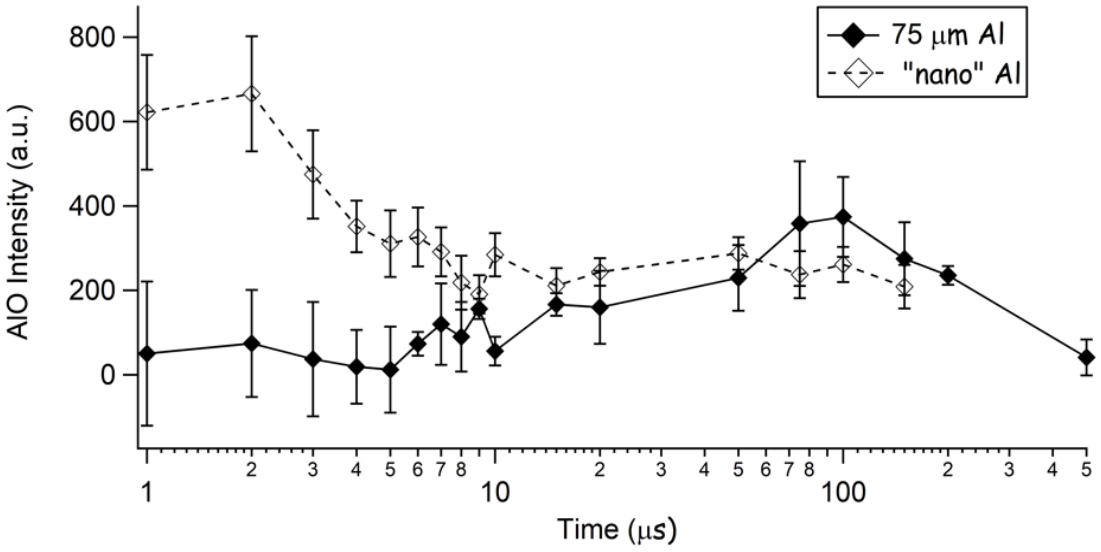

Fig. 4 Time-resolved AlO emission intensities for the nanopowder Al and <75 μm Al samples acquired with the ICCD spectrometer set to a 1-μs gate width and varying delay times (averaged over 20 laser shots at each delay time)

3.2 Middle-Time Energy Release

As shown in Fig. 4, following the cessation of the laser-induced plasma, AlO formation reaches a second maxima in the middle-time regime. We have attributed these peaks to particles directly ignited by the plasma. The time to peak AlO emission in this regime ranges from 40 μs for the 18-nm Al to 120 μs for the <75-mm Al and generally increases with increasing particle size and specific surface area (Fig. 5). The 18-nm Al is an outlier to the trend shown in Fig. 5, but it is also the sample with the most significant concentration of impurities (including the silicon-containing nanorods). In this time regime the strongly agglomerated 80-nm Al behaves similarly to the other nano-Al samples—the strong laser-induced shock wave may have de-agglomerated the ejected sample particles. Currently, we are investigating the relationship between the time to peak AlO emission in this regime and the contribution of Al reactions to Gurney velocities of explosive formulations.

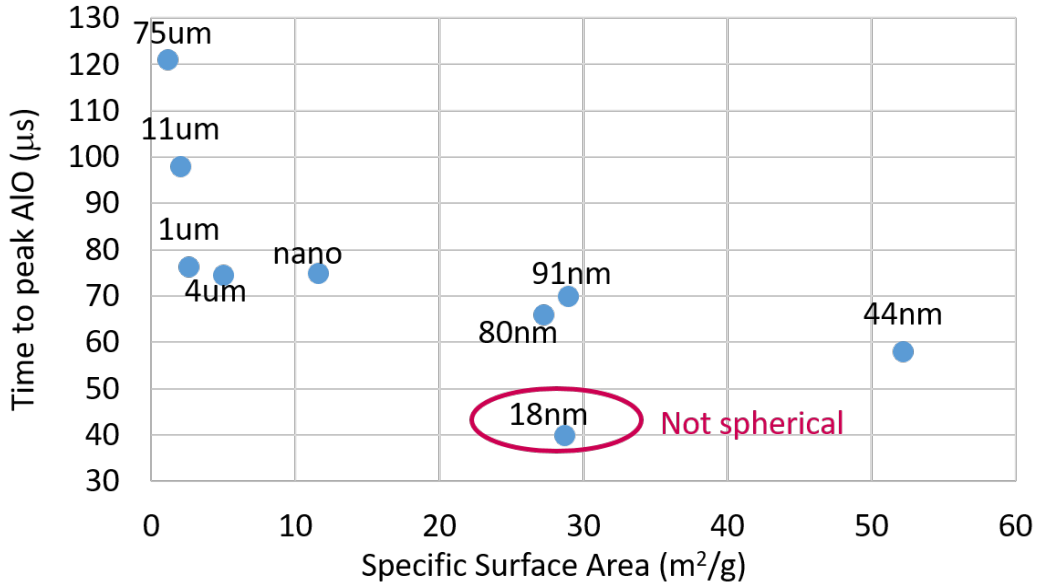

Fig. 5 Time to peak AlO emission intensities in the middle-energy release time regime as a function of specific surface area

3.3 Late-Time Energy Release

The late-time energy release of the Al particles was measured using photodiodes and a spectrometer to track the combustion emission. Unlike the laser-induced plasma emission spectra that result from the relaxation of excited species at temperatures exceeding 10,000 K, the combustion emission spectra are dominated by the blackbody emission from the solid burning particles and AlO emission at much lower temperatures (a few thousand K). The trends observed in the millisecond-timescale energy release are similar to those reported from conventional wire ignition-type combustion experiments for Al particles—namely, the combustion delay and the duration of the combustion are longer for larger particles.[13] Here, the high-heating-rate combustion behavior fell into three regimes based on particle size: 1) small particles (18 and 44 nm) burn out very quickly after the laser pulse, 2) intermediate particles (80 nm to 4 µm) experience a second ignition following the post-plasma combustion after a short delay, and 3) the larger particles (11 µm and <75 µm) have the longest burn times—and their burn time is strongly influenced by the amount of sample ejected into the air by the laser shock.

4. Methods for Catalyzing Aluminum Oxidation

In addition to studying the influence of Al particle properties on the microsecond-timescale energy release, we have been using LASEM to investigate methods for accelerating the oxidation of Al particles on the microsecond-timescale in order to

enhance detonation performance. The following sections provide a brief overview of some of the most promising materials.

4.1 Metal Alloys

Mechanical alloying has been used to improve the physical and mechanical properties of metals such as a higher specific modulus, higher strength-to-weight ratio, and increased fatigue strength, temperature stability, or wear resistance.[14] Enhanced ignition and combustion properties from mechanochemically prepared reactive materials via reactive milling have also been demonstrated, particularly at high heating rates.[15] Alloys of Al and other metals such as Mg,[16,17] Li,[18] and Ti[19] have been shown to have reduced ignition temperatures compared to pure Al. The exothermic reactions and/or liquid eutectic effect (enabling penetration of the metal into the Al grain boundaries) of the faster reacting non-Al alloy component can facilitate the Al oxidation. Although this Al catalysis via alloying has been demonstrated for both combustion and hydrolysis applications, we recently demonstrated that both Sn[20] and Zr[21] catalyze the oxidation of Al on a detonation timescale as well. Other alloys of interest include Al-Li and Al-Si. Future work in this area involves finding the best alloy composition for microsecond-timescale energy release of Al and optimizing the metallized explosive formulation with an appropriate oxidizer.

4.2 Passivating with Carbon

In order to protect the nano-Al surface from formation of the native oxide layer, researchers have developed various methods to provide a protective layer on the particle surface. Park et al.[22] demonstrated the increased thermal stability of nano-Al coated with a 1–3 nm layer of carbon and suggested that carbon may be a suitable passivating agent. Since oxidation of the carbon coating produces gaseous products (CO, CO_2), aggregation of the Al products is reduced. We recently used laser ablation synthesis to generate nano-Al particles (~10 nm) coated in carbon, with no oxide layer.[23] The microsecond-timescale energy release of these materials was significantly higher than that observed from commercial nano-Al. Because both the Al and the C can scavenge O from the reacting explosive at the crucial detonation timescale (thus decreasing detonation performance), optimization of an appropriately oxidized formulation is underway.

4.3 Coating with Oxygen-Containing Species

As an alternative to merely replacing the native oxide layer with a passivation coating, the surface of the Al particle can be functionalized such that the exothermic

reactions of the surface groups catalyze the reaction of the Al despite the presence of the alumina shell (e.g., Kappagantula et al.[24]). Using LASEM, we have recently demonstrated that both wrapping the Al particles in graphene oxide[25] and functionalizing the Al surface with aluminum iodate hexahydrate[11,26] can be used to facilitate the oxidation of Al on the microsecond-timescale. Because these materials contain O, increased detonation-timescale performance was observed with simple formulations of the metal additive and TNT.

5. Conclusions

While factors such as oxygen balance, explosive particle size, and binder properties may influence the detonation performance of aluminized explosives, our results show that microsecond-timescale energy release from pure nano-Al depends not just on particle size or specific surface area, but also on the active Al content. These properties are well known to vary from lot to lot—thus complete characterization of nano-Al samples is necessary prior to interpretation of results from detonative experiments. While numerous Al-containing additives have been developed that demonstrate significant promise for enhancing detonation performance, potential candidate materials to replace micron-Al for military applications must 1) have a reproducible synthesis process, 2) demonstrate long-term stability under ambient conditions, 3) be scalable to larger quantities, 4) be successfully formulated with current or future military explosives with no safety or environmental hazards, and 5) demonstrate enhanced detonation performance in conventional full-scale detonation tests.

6. References

1. Gottfried JL, Bukowski EJ. Laser-shocked energetic materials with metal additives: evaluation of chemistry and detonation performance. Appl Opt. 2017;56(3):B47–B57.

2. Brousseau P, Anderson CJ. Nanometric aluminum in explosives. Propellants Explos Pyrotech. 2002;27(5):300–306.

3. Zhou ZQ, Chen JG, Yuan HY, Nie JX. Effects of aluminum particle size on the detonation pressure of TNT/Al. Propellants Explos Pyrotech. 2017;42(12):1401–1409.

4. Liu D, Chen L, Wang C, Wu J. Aluminum acceleration and reaction characteristics for aluminized CL-20-based mixed explosives. Propellants Explos Pyrotech. 2018;43(6):543–551.

5. Vadhe PP, Pawar RB, Sinha RK, Asthana SN, Rao AS. Cast aluminized explosives. Combust Explos. 2008;44(4):461–477.

6. Sabourin JL, Yetter RA, Asay BW, Lloyd JM, Sanders VE, Risha GA, Son SF. Effect of nano-aluminum and fumed silica particles on deflagration and detonation of nitromethane. Propellants Explos Pyrotech. 2009;34(5):385–393.

7. Gottfried JL. Influence of exothermic chemical reactions on laser-induced shock waves. Phys Chem Chem Phys. 2014;16:21452–21466.

8. Gottfried JL. Laboratory-scale method for estimating explosive performance from laser-induced shock waves. Propellants Explos Pyrotech. 2015;40(5):674–681.

9. Densmore JM, Homan BE, Biss MM, McNesby KL. High-speed two-camera imaging pyrometer for mapping fireball temperatures. Appl Opt. 2011;50(33):6267–6271.

10. Dean SW, McNesby KL, Benjamin RA. High dynamic range imaging of energetic events. Joint Army Navy NASA Air Force (JANNAF) 41st Propellant and Explosives Development and Characterization (PEDCS); 2018 Dec 10–13; Vancouver, WA.

11. Gottfried JL, Smith DK, Wu C-C, Pantoya ML. Improving the explosive performance of aluminum nanoparticles with aluminum iodate hexahydrate (AIH). Sci Rep. 2018;8:8036.

12. Collins ES, Gottfried JL. Laser-induced deflagration for the characterization of energetic materials. Propellants Explos Pyrotech. 2017;42(6):592–602.

13. Yetter RA, Risha GA, Son SF. Metal particle combustion and nanotechnology. Proc Combust Inst. 2009;32(2):1819–1838.

14. Suryanarayana C. Mechanical alloying and milling. Prog Mater Sci. 2001;46 (1-2):1–184.

15. Dreizin EL, Schoenitz M. Mechanochemically prepared reactive and energetic materials: a review. J Mater Sci. 2017;52(20):11789–11809.

16. Shoshin YL, Mudryy RS, Dreizin EL. Preparation and characterization of energetic Al-Mg mechanical alloy powders. Combust Flame. 2002;128(3):259–269.

17. Aly Y, Dreizin EL. Ignition and combustion of Al·Mg alloy powders prepared by different techniques. Combust Flame. 2015;162(4):1440–1447.

18. Zhu X, Schoenitz M, Hoffmann VK, Dreizin EL. Reactive AI-Li powders prepared by mechanical alloying. Multifunctional Energetic Materials. 2006;896:39–44.

19. Shoshin YL, Trunov MA, Zhu X, Schoenitz M, Dreizin EL. Ignition of aluminum-rich Al–Ti mechanical alloys in air. Combust Flame. 2006;144(4):688–697.

20. Gottfried JL, Giri A. Unpublished work. Aberdeen Proving Ground (MD): CCDC Army Research Laboratory (US); 2019.

21. Wainwright ER, Dean SW, Lakshman SV, Weihs TP, Gottfried JL. Evaluating compositional effects on the laser-induced combustion and shock velocities of Al/Zr-based composite fuels. Combust Flame. 2019;213:357–368.

22. Park K, Rai A, Zachariah MR. Characterizing the coating and size-resolved oxidative stability of carbon-coated aluminum nanoparticles by single-particle mass-spectrometry. J Nano Res. 2006;8:455–464.

23. Davari SA, Gottfried JL, Liu C, Ribeiro EL, Duscher G, Mukherjee D. Graphitic-coated Al nanoparticles manufactured as superior energetic materials via laser ablation synthesis in organic solvents. Appl Surf Sci. 2019;473:156–163.

24. Kappagantula KS, Farley C, Pantoya ML, Horn J. Tuning energetic material reactivity using surface functionalization of aluminum fuels. J Phys Chem C. 2012;116(46):24469–24475.

25. Jiang Y, Deng S, Hong S, Zhao J, Huang S, Wu C-C, Gottfried JL, Nomura K-i, Li Y, Tiwari SC, Kalia RK, Vashishta P, Nakano A, Zheng X. Energetic performance of optically activated aluminum/graphene oxide composites. ACS Nano. 2018;12:11366–11375.

26. Miller KK, Gottfried JL, Walck SD, Pantoya ML, Wu C-C. Plasma surface treatment of aluminum nanoparticles for energetic material applications. Combust Flame. 2019;206:211–213.

List of Symbols, Abbreviations, and Acronyms

Al	aluminum
AlO	aluminum monoxide
ARL	Army Research Laboratory
BET	Brunauer–Emmett–Teller
DLS	dynamic light scattering
DSC-TGA	differential scanning calorimetry and thermogravimetric analysis
FTIR	Fourier transform infrared
ICCD	intensified charge-coupled device
LASEM	laser-induced air shock from energetic materials
LIBI	laser-induced breakdown ignition
LIBS	laser-induced breakdown spectroscopy
PMT	photomultiplier tube
SEM	scanning electron microscopy
TEM	transmission electron microscopy
TNT	trinitrotoluene

1 (PDF)	DEFENSE TECHNICAL INFORMATION CTR DTIC OCA
1 (PDF)	CCDC ARL FCDD RLD CL TECH LIB
4 (PDF)	CCDC ARL FCDD RLW LB J GOTTFRIED S DEAN C-C WU F DELUCIA